NUCL SCI TECH (2017) 28:120
DOI 10.1007/s41365-017-0273-0

Simulation study of slow extraction for the Shanghai Advanced Proton Therapy facility

Yu-Hui Yang[1,2] · Man-Zhou Zhang[1] · De-Ming Li[1]

Received: 24 November 2016 / Revised: 20 March 2017 / Accepted: 23 March 2017 / Published online: 2 August 2017

Abstract The Shanghai Advanced Proton Therapy facility employs third-integer slow extraction. In order to achieve accurate treatment, high-quality spill is needed. Therefore, parameters that may affect slow extraction should be investigated by simulation. A computer model of the synchrotron operation slow extraction was constructed with MATLAB®. By simulating the motion of the circulating protons, we could quantify the influence of machine and initial beam parameters on properties of the extracted beam, such as ripple, uniformity, stability, on- and off-time of the spill and spill width in the synchrotron. Suitable design parameters including the horizontal tunes, power supply ripple, longitudinal RF cavity voltage, RF-KO and the chromaticities were determined.

Keywords Slow extraction · Accelerator model · Spill ripple · Particle beam therapy · Synchrotron

1 Introduction

As a proton beam with sufficient initial kinetic energy penetrates a medium, its stopping power, the energy transferred on average by a proton to the medium through scattering electrons per unit distance into the medium, when plotted against distance penetrated, follows a Bragg curve [1]. Protons can significantly improve the effectiveness of radiotherapy while reducing damage to normal tissue over that of high-energy photons or electrons owing to a (Bragg) peak close to the end of the stopping power curve. Because of this, proton therapy has become an advanced and effective cancer treatment and a number of proton therapy centers have been constructed in recent years in the world. The Shanghai Advanced Proton Therapy (SAPT) facility is the first proton therapy facility designed by China. It will be installed at the end of 2016, and beam commissioning will commence in 2017. The accelerator consists of a 7-MeV injector, a 70- to 250-MeV synchrotron and transport beam lines to three treatment rooms (in Phase I). Spot scanning is used in the fixed beam and gantry rooms.

In order to meet the treatment requirements, third-integer resonant slow extraction from the synchrotron was used. The fractional part of the tune in the extraction plane, the horizontal, is close to 1/3 or 2/3. The resonance is driven by sextupoles, forming a set of closely overlapping triangles in horizontal phase space where a particle's motion is 'stable' (not resonant). The size and position of a triangle, termed as separatrix, depends on the particle's momentum and the machine's dispersion and chromaticity. Outside the triangle, the motion is unstable (resonant) and can be used to extract the beam. For clarity, 'separatrix' or 'triangle' refers to that belongs to a particle at the 'design' momentum. By using a transverse electric field oscillating at a certain frequency produced by a Radio Frequency Knock-Out (RF-KO) exciter, the beam emittance was increased gradually [1, 2]. When a particle's tune (here the horizontal) is on a resonance which is created by the layout

This work was supported by the Youth Innovation Promotion Association of Chinese Academy of Sciences (No. 20150210).

✉ Man-Zhou Zhang
zhangmanzhou@sinap.ac.cn

1 Shanghai Institute of Applied Physics, Chinese Academy of Sciences, Jiading Campus, Shanghai 201800, China

2 University of Chinese Academy of Sciences, Beijing 100049, China

and powering of the optics in a ring machine, in this case with a fractional part of 1/3 or 2/3, it enters the unstable region and reaches the septum in a few to several tens of turns around the machine.

To target a tumor accurately, many specific requirements should be met. First, a uniform stable and long (typically longer than ~ 1 s) spill to the tumor is required, which can be met by spill delivery systems [3–5]. For this design, a high uniformity means the spill must remain almost the same during the (whole) extraction when the 'sampling' rate (the reciprocal of the bin size of the spill's histogram) is 100 Hz. Similarly, high stability is in this instance a spill which is almost constant during the whole process of beam delivery when measured with considerably higher sampling rate of 10 kHz. The former is used for uniform scanning, and the latter for spot scanning. Such definitions of overall spill quality were used before [6]. Another requirement is the time it takes to switch the spill off during spot scanning of the proton beam. Many parameters and disturbances of slow extraction will affect the quality of the spill's time structure, such as RF-KO amplitude, RF-KO sweep frequency range and sweep period, sextupole strength, horizontal tune, voltage of the RF cavity, power supply ripple and beam momentum spread [7, 8]. The influence of different factors on quality of the spill is simulated in this paper.

These parameters affect the delay in stopping the spill caused by third-integer slow extraction after the RF-KO signal is suddenly switched off [9, 10]. A fast quadrupole magnet, as an auxiliary switch to avoid this delay, has been demonstrated to function very well [11]. This is achieved by quickly turning on the fast quadrupole magnet after the RF-KO is switched off. The resulting rapid shift in the horizontal tune enlarges the separatrix, thus avoiding that particles enter the unstable region, even when the region fluctuates due to fluctuation in the horizontal tune caused by power supply ripple and the longitudinal RF. However, it will introduce a short-lived but large ripple when the fast quadrupole is turned off. A single frequency of RF-KO is introduced to reduce this effect [12].

2 Slow extraction and design of tracking model

As shown in Fig. 1, the synchrotron includes a longitudinal RF cavity, six defocusing quadrupoles, six focusing quadrupoles, eight dipoles, the sextupoles for exciting the resonance (RSF and RSD), the sextupoles for controlling the chromaticity (SD and SF), a transverse excitation electrode (the RF-KO exciter/kicker, RFK) [13], an electrostatic septum (ES), a magnetic septum (MS) [14] and a fast quadrupole for fast tune switch. The three families of magnets, namely the dipole, the focusing quadrupole and

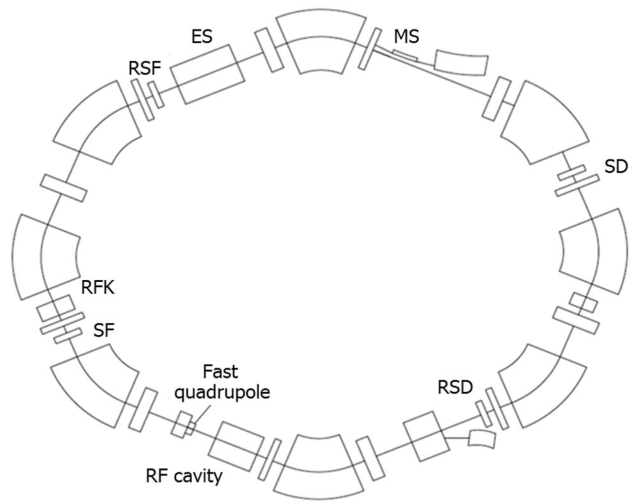

Fig. 1 Schematics of the SAPT synchrotron. Drawn to scale. Circumference = 24.6 m, $r = 1.4$ m, and $\gamma_t = 1.576$

the defocusing quadrupole, are individually connected in series.

There are no steerers for producing closed orbit bumps at the ES and MS, since extraction is possible without them at proton kinetic energies up to 250 MeV. Owing to symmetry of the optics, we can change the resonance strength without changing the chromaticity when the strengths of resonance sextupoles are equal or opposite, i.e., $S(\mathrm{RSD}) = -S(\mathrm{RSF})$. And vice versa, when $S(\mathrm{SD}) = S(\mathrm{SF})$ we can change the chromaticity only. The RF cavity operates at a single frequency which is at the harmonic $h = 1$ of the circulating beam's revolution frequency.

The third-integer slow extraction is a nonlinear system and is influenced by various factors. For this reason, a large number of (macro) particles shall be tracked. To ensure the simulation accuracy, ~ 10 treatment spots or more are required. Each spot is produced by a spill 'shot' of 0.1-ms duration. This means tracking 10^5 macroparticles for 10^6 turns. Since there are over 100 accelerator components required by CERN's MAD [15] code, the AT [16] library from SLAC or other commonly used particle tracking simulation—and a single tracking scenario may require hundreds of hours with dozens of scenarios factors for producing plots to reveal trends in parameter dependencies—it is difficult to complete the simulation surveys without developing a new tracking model.

The calculation time can be reduced by limiting the number of accelerator components and adding parallel computation. The simplest model employs a transverse single turn transfer matrix (neglecting the coupling between the transverse and longitudinal motion, a third-integer resonance occurs only in the transverse direction) and the thin elements of RFK, a virtual sextupole and RF cavity. The drawbacks of this model are exclusion of the dispersion effect and the approximation of synchrotron oscillations of protons. Also, the horizontal chromaticity and resonance strength cannot be changed separately.

An alternative model is constructed by dividing the ring into segments and setting the real sextupoles, situated between segments, in such a way that they cause minimal beam loss at the extraction septum. The transfer matrices are for segments of the beamline containing only linear optical elements, that is, the dipole and quadrupole magnets. The only remaining drawback here is that chromaticity is unaccounted for.

The two models, and a more computationally intensive yet accurate model implemented using the AT library, were constructed with the numerical scripting language MATLAB. Figure 2 shows the particles tracked with the same RF-KO signal by the three models. The phase space ellipses start to move outwards from the center due to the RFK excitation. The red, green and blue points are from, respectively, the AT, segmented transmission matrix and single turn transmission matrix models. The AT was designed to simulate electron beams in synchrotrons and beamlines. After a few modifications to the RF cavity, the longitudinal and transverse dynamics were suitable for protons. The AT results agreed well with those of the segmented model, but the segmented model was much faster than the AT model because we did not need to calculate matrix-based particle ‘kicks’ for each magnet per turn. So we chose the segmented model to do the subsequent simulations. Figure 3 shows the transverse phase space of how a single particle, under the dominant effect of the sextupoles and the weaker effect of the RF-KO, spirals outwards from just outside a corner of the separatrix to the electrostatic septum ES, returning to an arm of the separatrix every three turns.

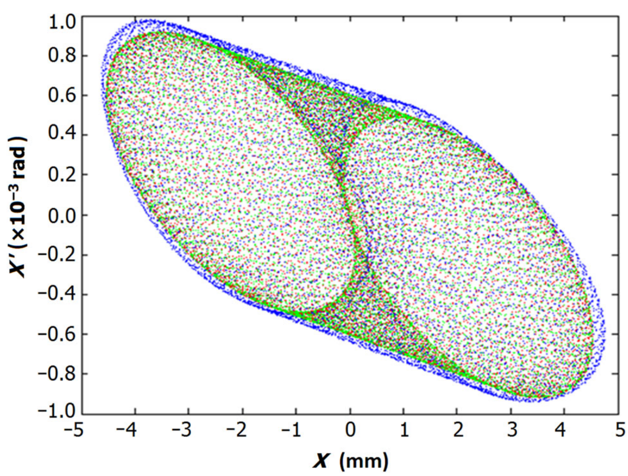

Fig. 2 (Color online) Phase space distributions of 70 MeV protons after 1000 turns simulated with the AT (*red points*), segmented transmission matrix (*green points*) and single turn transmission matrix (*blue points*) models. Peak deflection by RFK is 2 urad, RF cavity is 200 V, no resonance is powered by the sextupoles, and normalized momentum spread prior to turning the RF cavity on is $d = 0.1‰$ and is Gaussian distributed with cuts at 3σ

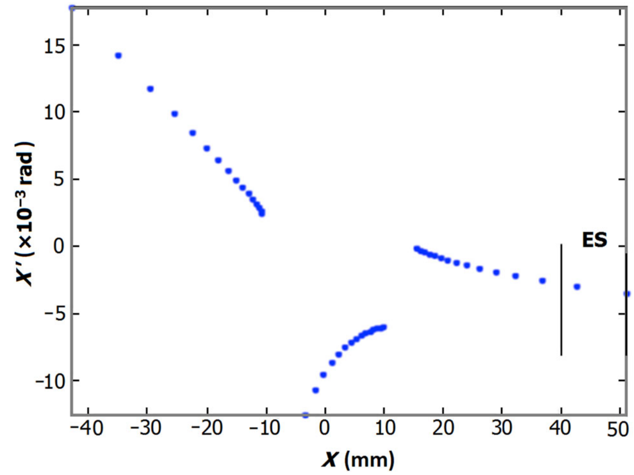

Fig. 3 (Color online) Phase space trajectory of a 70 MeV proton during RF-KO. Aperture of the electrostatic septum (ES) is marked. Septum mechanical angle is -3 mrad. ES is located at 40 mm from the designed orbit and toward the center of the synchrotron

Dual frequency modulation (FM) is used to generate the beam excitation voltage form for the RFK. Two triangular sweeping frequencies with a phase difference of 180° and the same carrier frequency are superimposed. These FMs cover the (horizontal) betatron frequencies of particles located in the area within the separatrix, which consists of outer ‘extraction’ and an inner ‘diffusion’ area. Strictly speaking, there is a partial overlap between the two areas. When one sweeping frequency signal is extracting, the other is diffusing the beam, and vice versa, thereby creating a continuous extraction [17–19]. During extraction at constant RF-KO voltage amplitude, the intensity of the beam in the ring decreases with increasing time. To maintain spill uniformity, the RF-KO amplitude should be modulated to regulate the rate of growth of the beam emittance in the ring, which in turn changes the spill’s time structure making it uniform [3, 4].

The addition of the fast quadrupole magnet changes the transfer matrix of the accelerator and hence the need of constructing two sets of transfer matrix. One set contains the fast quadrupole, the other set does not (a drift length replaces this quadrupole), and switch of the fast quadrupoles can be simulated by switching between the two sets of transfer matrix. Because there is a large spill in a short time at the beginning of extraction process, this large spill can be replaced by the more stable spill after it treats tumors [20]. A simulated spill includes the initial large spill which would normally be ‘pre-extracted.’ The simulation results correspond to the more stable pre-extracted spill.

Table 1 shows typical analysis conditions used in the simulation in this paper. As mentioned above, the

Table 1 Typical analysis conditions

Parameters	Momentum spread (1σ, 3σ cut)	Horizontal tune (Q_h)	RF cavity voltage	Chromaticity	Resonance sextupoles strength (S)	Proton energy
Design values	0.3‰	1.6802	200 V	−1.5	12.5 $m^{-1/2}$	70–250 MeV

Horizontal dispersion at entrance to the ES is 2.4 m

Table 2 Extraction widths at different resonance sextupoles strengths, with horizontal tune of 1.6802

Strength (S $m^{-1/2}$)	10.0	12.0	12.5	13.0	14.0	18.0
Width (mm)	4.0	8.6	10.1	11.3	14.7	27.3

resonance sextupole strength is that applied to both resonance sextupoles.

In what follows, some parameters are changed from their design values. $S = \beta_x^{3/2}(\mathrm{d}^2B_z/\mathrm{d}x^2)(l_{\mathrm{eff}}/B_\rho)/2$ is the normalized sextupole strength of a sextupole magnet, where B_ρ is the magnetic rigidity, β_x is the horizontal betatron function at the sextupole, and l_{eff} is the effective length of the magnetic field.

3 Factors that influence extraction efficiency

The horizontal tune of the synchrotron and the strength of the resonance sextupoles may affect greatly the width of the spill. The cathode and anode of the electrostatic septum are gapped at just 10 mm, and this spill can be lost in the electrodes. The width of the extracted beam will therefore affect the extraction efficiency [21].

The normalized sextupole strength $S = 12.5\ \mathrm{m}^{-1/2}$ ($l_{\mathrm{eff}} = 0.1$ m for each resonance sextupole) is the most preferable of those in Table 2 because the extraction width is, relative to the others, reasonable and the spill losses should therefore be small.

Beam momentum spread has an impact on the transverse motion through dispersion and chromaticity, which leads to the resonance triangle moving and scaling, respectively. The extraction width increases with the momentum spread and hence a larger number of particles to go beyond the electrostatic septum boundary, i.e., a larger loss. The momentum spread normalized to the mean momentum was 0.3‰ (σ). With a change of 1‰, the extraction width increases by >60%, so large momentum spread should be avoided.

4 Uniformity analysis of the spill

In order to realize a uniform extraction of the beam, the simulation required amplitude modulation (AM) of the RF-KO beam excitation voltage, because the momentum spread and the horizontal tune of the synchrotron have influence on the uniformity of the spill and the number of particles extracted. Spill amplitude variation <30% of the average over a region of interest—namely the pre-extracted spill indicated by the box in Fig. 4, for example—is required according to studies by the treatment group. In the time of almost a full course of treatment, we simulated the effects of different momentum spread and horizontal tune on the spill amplitude (the maximum deviation of the instantaneous spill current from the average over the pre-extracted spill) and beam transmission (the beam fraction coming out of the machine at the end of extraction and failing to hit any apertures in the ring including the ES) under the same AM condition.

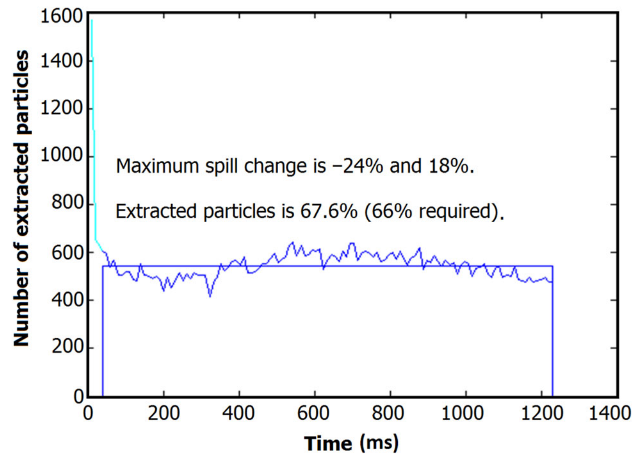

Fig. 4 (Color online) Spill versus time. Protons extracted at 70 MeV from the SAPT synchrotron per 10 ms bin (time between points), i.e., the spill versus time during a continuous-extraction RF-KO cycle. Initial number of macroparticles was 10^5. Here, the first 2000 macroparticles would be 'dropped' in practice, instead of being delivered to the treatment rooms. The average spill over 40–1240 ms is overlaid

A change in the momentum spread affects the extracted beam width. A vibrating change in the amplitude of resonance triangle caused by power supply ripple leads to a change in flow of the spill. From Table 3, the spill amplitude and transmission change considerably less when the momentum spread is 0.2–0.4‰.

When the horizontal tune (Q_h) is too close to the resonance, a slight variation of it can affect: (1) the range of stable circulating beam; (2) the step width for a particle to enter the ES; and (3) the time to reach the ES once a

Table 3 Maximum change in spill amplitude and beam transmission at different momentum spreads, at the horizontal chromaticity of −1.5

Momentum spread (1σ, 3σ cut) (‰)	0.2	0.3	0.4	1
Maximum change in spill amplitude (peak/mean) (%)	24	24	20	36
Transmission of protons (%)	63.9	67.6	69.5	72.1

Table 4 Maximum change in spill amplitude and beam transmission at horizontal tune values of around 5/3

Horizontal tune (Q_h)	1.67	1.677	1.6792	1.6802	1.6810
Maximum variation of spill amplitude (%)	211	47	27	24	21
Transmission of protons (%)	90.5	61.1	68.6	67.6	68.2

Table 5 Maximum spill ripples at different horizontal chromaticities

Horizontal chromaticity	0.00	−0.20	−0.50	−0.75	−1.00	−1.50	−3.00	−4.50
Maximum spill ripple (R, %)	67	56	43	34	28	24	24	24

particle becomes unstable. All these affect extraction of the spill. When the horizontal tune is too far from the resonance, the resonance triangle will be deformed due to the excessive resonance sextupole strength, which is big perturbation to the optics under such conditions. So, a suitable horizontal tune is chosen at $Q_h = 1.68$. From Table 4, when the Q_h changes by less than ± 0.001, the spill quality changed little, but degrades increasingly rapidly as the Q_h approaches the resonance.

5 Stability analysis of the beam

Many factors can affect the stability of the spill $I(t)$, such as horizontal tune, power supply ripple and RF cavity voltage. The spill stability index R (or spill ripple) is defined as the RMS normalized to the mean, $R = (\langle I^2\rangle / \langle I_m^2\rangle - 1)^{1/2}$. Simulations by the treatment group show that a successful treatment requires the spill ripple of <40%.

Collective beam effects will be significant because the ca. 24.6 m circumference synchrotron shall deliver 4×10^{10}–8×10^{10} protons of 70–250 MeV in average beam radius of 1 cm. The chromaticity couples longitudinal and transverse motion and therefore affects the spill stability. Because of this and the fact that the synchrotron works below the transition energy, the chromaticity should be kept negative to avoid head–tail instabilities. The simulation results in Table 5 show that the spill ripple is small at great chromaticities. However, natural chromaticity shall be further considered.

Increasing the RF peak voltage in the cavity enhances the amplitude in the momentum of the longitudinal synchrotron oscillations and increases the synchrotron tunes of the proton beam, which may, if not excessive, restrain the ripple of the extracted beam. The spill stability was poor without cavity voltage; in particular, the maximum spill ripple was 78% with no power supply ripple. Furthermore, the peak voltage at 50–1000 V had relatively little effect on the spill ripple, as the spill ripple was in the range of just 20–30% (Fig. 5).

The horizontal tune is a decisive factor governing the third-integer resonance's effect on the beam, and ripple in the power supplies to the bends and quadrupoles affects the horizontal tune, which in turn affects the number of spiral steps along the extraction arm of the separatrix, and a particle undergoes until it arrives at the ES. Thus, there is a great influence on the stabilization of the extracted beam, which was confirmed by many simulations.

To simulate the quadrupole power supply ripple, we used a sinusoidal waveform, at 1 kHz, to simulate the power supply ripple. A 1-kHz ripple was thus imposed each of the two main quadrupole power supplies with a random phase difference between them (one supplies the horizontally focusing quadrupoles, and the other the horizontally defocusing quadrupoles). The bend power supply ripple was equivalent to and in-phase with the quadrupole power supply ripple. The phase between the two power supply ripples was constant in each extraction. Extractions in different phase difference were simulated to get an average effect. We simulated the effect of the power supply ripple on the spill for different RF cavity voltages. The results of the bending magnets in Fig. 5a are similar to those of the power supply ripple in the quadrupoles in Fig. 5b. At RF cavity voltage of 100 V, the spill ripple reduced a lot for large power supply ripple.

However, when the power supply ripple frequency was changed to 2 kHz, it was similar to the other RF cavity voltages. This shows that in different cavity voltages, a

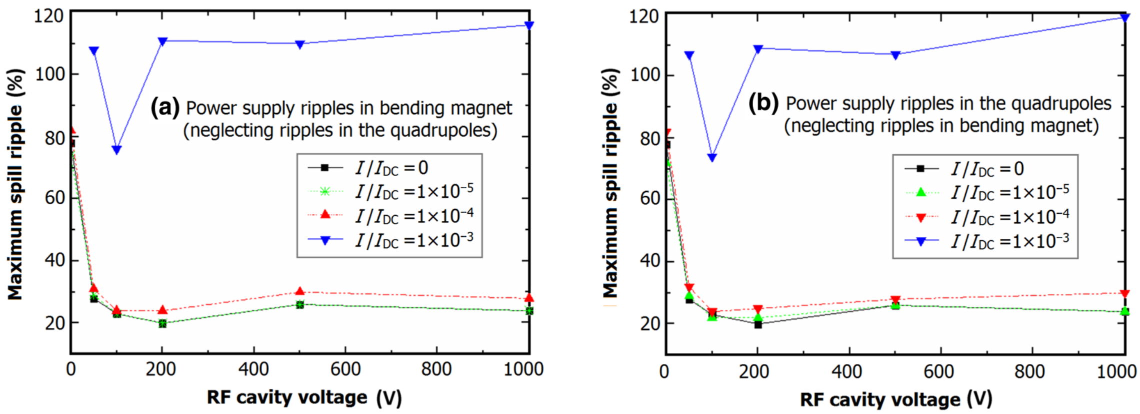

Fig. 5 (Color online) Maximum power supply ripple in the bending magnet (**a**) and quadrupoles (**b**) at 70 MeV as a function of RF cavity voltage, for $I/I_{DC} = 0$, 1×10^{-5}, 1×10^{-4} and 1×10^{-3} where I_{DC} is the DC part of the power supply current

good match of longitudinal oscillation frequency and power supply ripple could reduce the spill ripple effectively. Too much power supply ripple would lead to spill instability, but the power supply ripple to which the beam is subjected is less than $\sim 10^{-4}$. Our design meets the requirement for spill ripple <40%.

Other parameters which may affect the spill ripple were simulated. The slight fluctuation of RF-KO scanning frequency had little effect on the spill stability, and the effect of momentum spread on the spill ripple was not obvious.

6 Fast switch for the spill

Spot scanning requires frequent switching of the spill by switching the RF-KO on and off. Figure 6 shows a switched spill we simulated. The fall-time in the spill, referred to as 'off-time,' is much more important than rise-time, i.e., 'on-time,' because in general the on-time is too short to be of concern [22]. Therefore, we focused on the rapid turnoff of the spill.

Although the voltage of the RF cavity was suppressed the spill ripple, the synchrotron oscillations kept moving particles into the unstable area, hence the prolonging the spill off-time. As shown in Fig. 7, the spill off-time increased at 0 V of the RF cavity voltage and reduced after the cavity voltage was about 50 V. So, the RF cavity voltage can be ≥50 V.

To achieve a rapid shutdown, a fast quadrupole was added so that the spill off-time could be reduced to <0.2 ms. In order to suppress the initial spike in the spill produced by the fast quadrupole as it shifted the horizontal tune back to the extraction setting, a single frequency signal was added in the simulation to the dual FM signal of the RF-KO exciter. It was found that the inhibition was strongest when the frequency was at the edge of the resonance region and the maximum deflection was 1 urad. The effect was clearly visible.

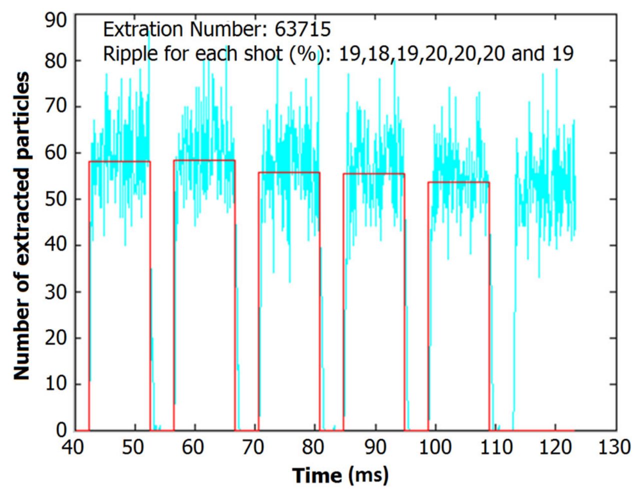

Fig. 6 (Color online) Spill versus time, at 70 MeV. The RF-KO was switched on and off, to produce 5 spill shots over the time frame in the abscissa (during an RF-KO cycle). Ordinate represents the number of protons extracted per 0.1 ms bin. The *red boxes* are the average spill during a shot

Power supply ripple extends the spill off-time, so the same fast quadrupole is needed to overcome this negative effect. When the power supply ripple in the main-quadrupoles was 10^{-4}, which is the maximum in the design, and the RF cavity peak voltage was 200 V, the horizontal tune should be increased by at least 0.0011 to ensure an off-time of <0.2 ms. However, a large fast quadrupole strength results in a large instantaneous spill, and a large spill ripple [23]; when the fast quadrupole made the horizontal tune increase by 0.0015, the spill ripple would increase up to the tolerance limit of 40%.

The fast quadrupole focusing strength can be determined from changes observed in the horizontal tune.

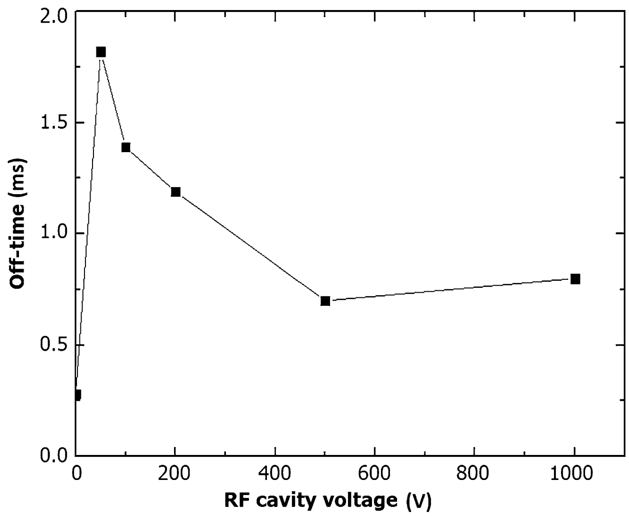

Fig. 7 Off-time versus the RF cavity voltage at 70 MeV of proton energy

7 Conclusion

A tracking model of the Shanghai Advanced Proton Therapy synchrotron was constructed by dividing the synchrotron into segments and replacing the transfer matrices in each segment by a single matrix for reducing the computation time and applying the chromaticity with just sextupole magnets in order to represent the 'missing' natural chromaticity as well as that introduced by the sextupoles. With this setup, we could simulate the effects of factors such as horizontal tune, RF cavity voltage, power supply ripple, circulating beam momentum spread and fast quadrupole induced tune shifts on the system. We have verified the effect of these factors on the efficiency, uniformity and stability of the spill, and with it, have established optimal control parameters of the slow extraction system. In addition, the design helped realize fast switching of the spill, which met the needs of the therapy. It may also serve as a reference for commissioning the accelerator.

References

1. P.J. Bryant, L. Badano, M. Benedikt et al., Proton-ion medical machine study (PIMMS). CERN (1999). doi:10.1007/bf03038873
2. T. Furukawa, K. Noda, M. Muramatsu et al., New approach toward optimized resonant slow-extraction. Nucl. Instrum. Meth. A **515**, 853–861 (2003). doi:10.1016/j.nima.2003.07.036
3. T. Furukawa, K. Noda, M. Muramatsu et al., Global spill control in RF-knockout slow-extraction. Nucl. Instrum. Meth. A **522**, 196–204 (2004). doi:10.1016/j.nima.2003.11.395
4. T. Furukawa, K. Noda, T.H. Uesugi et al., Intensity control in RF-knockout extraction for scanning irradiation. Nucl. Instrum. Meth. B **240**, 32–35 (2005). doi:10.1016/j.nimb.2005.06.083
5. K. Mizushima, S. Sato, T. Shirai et al., Development of beam current control system in RF-knockout slow extraction. Nucl. Instrum. Meth. B **269**, 2915–2918 (2011). doi:10.1016/j.nimb.2011.04.039
6. M. Kirk, D. Ondreka, P. Spiller, SIS-18 RF knock-out optimization studies, in *Proceedings of IPAC* (2013). ISBN 978-3-95450-122-9
7. S. Dan, L.H. Ouyang, M. Gu, The RF-knockout slow-extraction for Shanghai proton therapy facility. Nucl. Tech. **35**(3), 231–235 (2012). **(in Chinese)**
8. K. Mizushima, T. Shirai, T. Furukawa et al., Making beam spill less sensitive to power supply ripple in resonant slow extraction. Nucl. Instrum. Meth. A **638**, 19–23 (2011). doi:10.1016/j.nima.2011.02.056
9. T. Furukawa, K. Noda, Fast beam cut-off method in RF-knockout extraction for spot-scanning. Nucl. Instrum. Meth. A **489**, 59–67 (2002). doi:10.1016/s0168-9002(02)00895-1
10. T. Furukawa, K. Noda, E. Urakabe et al., Characteristics of fast beam switching for spot scanning. Nucl. Instrum. Meth. A **503**, 485–495 (2003). doi:10.1016/S0168-9002(03)01000-3
11. T. Nakanishi, T. Furukawa, K. Yoshida et al., Slowbeam-extraction method using a fast Q-magnet assisted by RF-knockout. Nucl. Instrum. Meth. A **553**, 400–406 (2005). doi:10.1016/j.nima.2005.07.023
12. K. Mizushima, T. Shirai, T. Furukawa et al., Reduction of uncontrollable spilled beam in RF-knockout slow extraction. Nucl. Instrum. Meth. A **606**, 325–329 (2009). doi:10.1016/j.nima.2009.05.154
13. F. Méot, High-precision simulation of slow-extraction spill from a hadrontherapy synchrotron. Nucl. Instrum. Meth. A **595**, 535–542 (2008). doi:10.1016/j.nima.2008.05.060
14. S. Sato, T. Furukawa, K. Noda, Dynamic intensity control system with RF-knockout slow-extraction in the HIMAC synchrotron. Nucl. Instrum. Meth. A **574**, 226–231 (2007). doi:10.1016/j.nima.2007.01.174
15. H. Grot, F Christoph Iselin, The MAD Program User's Reference Manual CERN/SL/90-13(AP)
16. A. Terebilo, Accelerator Toolbox for MATLAB, SLAC-PUB-8732
17. K. Noda, T. Furukawa, S. Shibuya et al., Source of spill ripple in the RF-KO slow-extraction method with FM and AM. Nucl. Instrum. Meth. A **492**, 241–252 (2002). doi:10.1016/s0168-9002(02)01318-9
18. K. Noda, T. Furukawa, S. Shibuya et al., Advanced RF-KO slow-extraction method for the reduction of spill ripple. Nucl. Instrum. Meth. A **492**, 253–263 (2002). doi:10.1016/s0168-9002(02)01319-0
19. K. Noda, M. Kanazawa, A. Itano et al., Slow beam extraction by a transverse RF field with AM and FM. Nucl. Instrum. Meth. A **374**, 269–277 (1996). doi:10.1016/0168-9002(96)00096-4
20. K. Mizushima, T. Furukawa, T. Shirai et al., Reliable beam-intensity control technique at the HIMAC synchrotron, in *Proceedings of IBIC* (2012). ISBN 978-3-95450-119-9
21. J. Shi, J.C. Yang, J.W. Xia, RF knock-out extraction in HITFiL. Chin. Phys. C **36**(10), 1004–1008 (2012). doi:10.1088/1674-1137/36/10/016
22. M. Pullia, Transit time for third order resonance extraction. CERN/PS 96-36 (DI), October 1996
23. T. Nakanishi, Dependence of a frequency bandwidth on a spill structure in the RF-knockout extraction. Nucl. Instrum. Meth. A **621**, 62–67 (2010). doi:10.1016/j.nima.2010.04.070